Skeletal Radiology
https://doi.org/10.1007/s00256-024-04720-5

SCIENTIFIC ARTICLE

Effects of axial loading and positions on lumbar spinal stenosis: an MRI study using a new axial loading device

Xingyu Fang[1,2,3] · Mengqiu Cui[1,2] · Yingwei Wang[2] · Lin Liu[3] · Wei Lv[3] · Huiyi Ye[2] · Gang Liu[2]

Received: 17 April 2024 / Revised: 1 June 2024 / Accepted: 3 June 2024

Abstract

Objective A new axial loading device was used to investigate the effects of axial loading and positions on lumbar structure and lumbar spinal stenosis.

Methods A total of 40 patients sequentially underwent 4 examinations: (1) the psoas-relaxed position MRI, (2) the extended position MRI, (3) the psoas-relaxed position axial loading MRI, (4) the extended position axial loading MRI. The dural sac cross-sectional area, sagittal vertebral canal diameter, disc height and ligamentum flavum thickness of L3-4, L4-5, L5-S1 and lumbar lordosis angle were measured and compared. A new device with pneumatic shoulder-hip compression mode was used for axial loading.

Results In the absence of axial loading, there was a significant reduction in dural sac cross-sectional area with extension only seen at the L3-4 ($p = 0.033$) relative to the dural sac area in the psoas-relaxed position. However, with axial loading, there was a significant reduction in dural sac cross-sectional area at all levels in both psoas-relaxed (L3-4, $p = 0.041$; L5-S1, $p = 0.005$; L4-5, $p = 0.002$) and extension ($p < 0.001$) positions. The sagittal vertebral canal diameter and disc height were significantly reduced at all lumbar levels with axial loading and extension ($p < 0.001$); however, in psoas-relaxed position, the sagittal vertebral canal diameter was only reduced with axial loading at L3-4 ($p = 0.018$) and L4-5 ($p = 0.011$), and the disc height was reduced with axial-loading at all levels (L3-4, $p = 0.027$; L5-S1, $p = 0.001$; L4-5, $p < 0.001$). The ligamentum flavum thickness and lumbar lordosis in extension position had a statistically significant increase compared to psoas-relaxed position with or without axial loading ($p < 0.001$).

Conclusion Both axial loading and extension of lumbar may exacerbate lumbar spinal stenosis. Axial loading in extension position could maximally aggravate lumbar spinal stenosis, but may cause some patients intolerable. For those patients, axial loading MRI in psoas-relaxed position may be a good choice.

Keywords axial loading · patient positioning · magnetic resonance imaging · spinal stenosis · lumbosacral region

Abbreviations

AlMRI	Axial loading magnetic resonance imaging
DH	Disc height
DSCA	Dural sac cross-sectional area
FOV	Field of view
FRFSE	Fast recovery fast spin-echo
FSE	Fast spin-echo
ICC	Intraclass correlation coefficient
LFT	Ligamentum flavum thickness
LSS	Lumbar spinal stenosis
SVCD	Sagittal vertebral canal diameter
TE	Echo time
TR	Repetition time

Huiyi Ye and Gang Liu these authors contributed equally contributed to this work.

✉ Huiyi Ye
13701100368@163.com

✉ Gang Liu
liugang301fsk@163.com

[1] Medical School of Chinese PLA, Beijing 100853, China

[2] Department of Radiology, The First Medical Center, Chinese PLA General Hospital, Beijing 100853, China

[3] Department of Radiology, the 305 Hospital of PLA, Beijing 100017, China

Published online: 07 June 2024

Introduction

Magnetic resonance imaging (MRI) is the best noninvasive examination for the diagnosis of lumbar spinal stenosis (LSS) because it provides excellent visualization of anatomical structures and soft tissue contrast [1, 2]. Previous studies have demonstrated that axial loading MRI could provide more diagnostic information, similar to that of upright lumbar spine MRI [3–6]. The axial loading device currently applied in clinical, is the "DynaWell L-Spine" (Dynawell Diagnostics, NY, USA). This device works by applying pressure through the shoulders and feet of the patient while the patient maintains a straight-leg position with a cushion placed beneath the low-back for stabilization [7, 8].

During the examination the patient's lumbar spine was actually in extended position which may also aggravate LSS [9, 10]. The design of this device, with a pillow beneath the low-back, requires the patient to be imaged in extension, which is a potential confounder when determining if it is axial-loading or extension eliciting the structural changes. We used a new lumbar spine axial loading device that applies pressure through the shoulders and hips. The new device could be used in two positions: lumbar spine extended position or psoas-relaxed position with knees flexion. In this study, we investigated a new axial-loading device that can be used in both psoas-relaxed and extension positions to determine the effects of extension, axial-loading, and a combination of these on the spinal morphology.

Materials and methods

Participants

This study was approved by the Institutional Review Board of the 305 Hospital of PLA and conducted in accordance with the Declaration of Helsinki (as revised in 2013). Written informed consent was obtained from all subjects. A total of 40 patients were included between January 2023 and July 2023. The inclusion criteria for the patients were: neurogenic intermittent claudication and/or radicular leg pain and/or numbness with a duration of at least 3 months. The exclusion criteria were: previous spinal surgery, severe osteoporosis, severe cardiopulmonary dysfunction, history of spinal fracture, spinal malignant tumor, lower limb disease, and claustrophobia.

Axial loading device

The new lumbar spine alMRI (axial loading MRI) device developed by our team consists of wearable components and pressure components, which can achieve axial loading of lumbar spine by exerting pressure on the shoulders and hips (Fig. 1A) [11, 12]. The pressure is applied in the pneumatic mode. The control system of the pressure component pneumatically pressurizes the cylinder connected to the wearable components through a long ventilation tube and tightens the piston to generate axial loading of the lumbar spine. The pressure

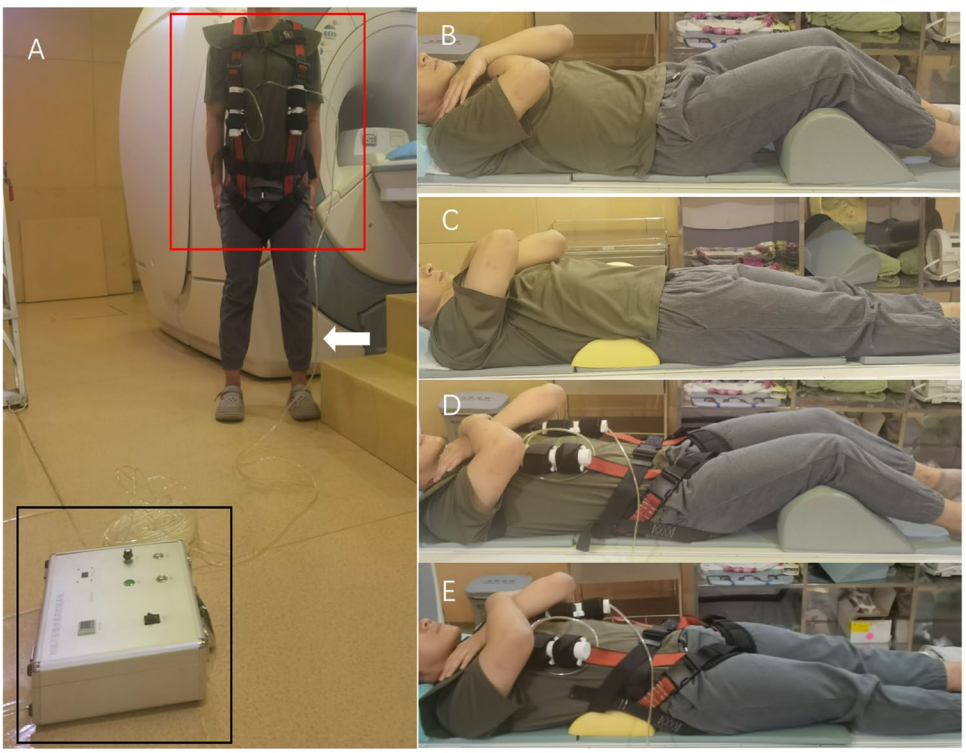

Fig. 1 The new axial loading MRI device (**A**) consists of wearable components (red box) and pressure components (black box). The control system pneumatically pressurizes the cylinder connected to the wearable components through the ventilation tube (arrow) and tightens the piston to generate axial loading of the lumbar spine. Patient underwent 4 MRI scanning protocols in sequence: rMRI (**B**), eMRI (**C**), r+alMRI (**D**) and e+alMRI (**E**). rMRI, psoas-relaxed position MRI; eMRI, extended position MRI; r+alMRI, the psoas-relaxed position axial loading MRI; e+alMRI, the extended position axial loading MRI

could be steadily applied and accurately measured through the control system remotely. The axial loading pressure is controlled to be equal to 40-50% of the patient's own body weight, simulating the load on lumbar spine when the body is upright, and the compression time was 5 minutes [13–15].

MRI protocol

All MRI examinations were performed on a 1.5-T system (Signa Optima, GE Medical Systems, Milwaukee, WI, USA) using a surface coil. Sagittal T2-weighted fast recovery fast spin-echo (FRFSE), T1-weighted fast spin-echo (FSE), short tau inversion recovery (STIR) and axial T2-weighted FRFSE were performed using a standard protocol (Table 1).

Imaging acquisition

Each patient underwent 4 MRI scanning protocols in sequence (Fig. 1B-E): (1) the psoas-relaxed position MRI (rMRI) with a cushion under the legs, (2) the extended position MRI (eMRI) with extended legs and a cushion under the lumbar spine, (3) the psoas-relaxed position axial loading MRI (r+alMRI) with a cushion under the legs, (4) the extended position axial loading MRI (e+alMRI) with extended legs and a cushion under the lumbar spine. The cushion under the lumbar spine was a thick memory foam of 60*30*15cm. The cushion under the legs was a thick hard foam of 80*50*30cm.

Patients underwent rMRI and eMRI on the first day, followed by r+alMRI and e+alMRI on the second day, and the two examinations each day were separated by 1 hour. The purpose of these arrangements was to exclude the effect of the previous scanning and to prevent patients from becoming fatigued and thus influencing the examinee comfort assessment. All scans were performed between 8:00 am and 10:00 am to minimize the effect if timepoint variations on the lumbar spine as much as possible [16].

Image quantitative measurements

The dural sac cross-sectional area (DSCA), sagittal vertebral canal diameter (SVCD), disc height (DH) and ligamentum flavum thickness (LFT) were measured at L3-L4, L4-L5, and L5-S1. Meanwhile, the lumbar lordosis angle (LA) was measured as L1-S1 angle on the mid-sagittal image (Fig. 2). The DSCA, SVCD and LFT were measured on the axial image. The DSCA was measured at each intervertebral space with

Table 1 Details of sequences of the lumbar spine MRI

Parameters	FRFSE T2 Sagittal	FSE T1 Sagittal	FRFSE T2 Axial	STIR Sagittal
TR, msec	2600	500	2600	3200
TE, msec	120	10	120	100
ST, mm	4	4	4	4
SI, mm	0.5	0.5	0.5	0.5
FOV, mm	320x420	320x420	200x260	320x420

TR repetition time, TE echo time, ST slice thickness, SI slice interval, NSA number of signal averaging, FOV field of view, FRFSE fast recovery fast spin-echo, FSE fast spin-echo, STIR short tau inversion recovery

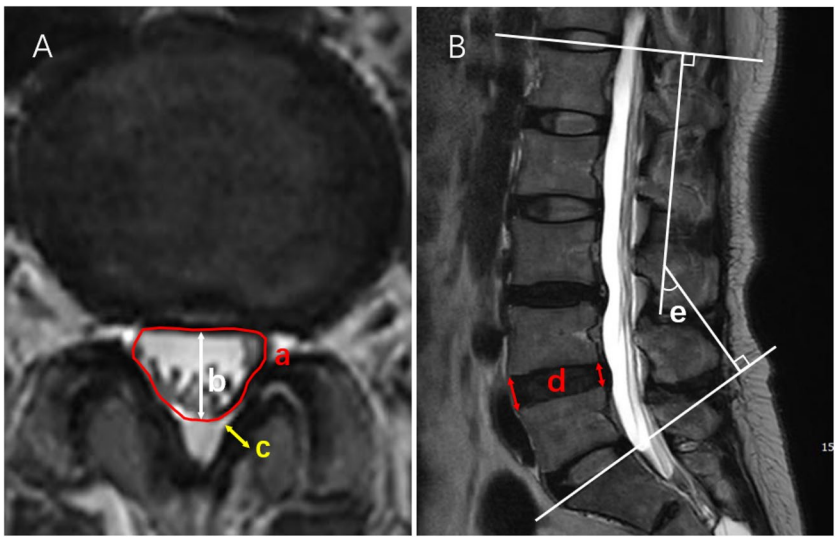

Fig. 2 Measurements of (**a**) DSCA, (**b**) SVCD and (**c**) LFT in an axial T2-weighted FRFSE image, (**d**) DH and (**e**) LA in T2-weighted FRFSE image. DSCA, dural-sac cross-sectional area; SVCD, sagittal vertebral canal diameter; DH, disc height; LFT, ligamentum flavum thickness; LA, lordosis angle; FRFSE, fast recovery fast spin-echo

the smallest area. The thickest part of the ligamentum flavum was selected for measurement. The SVCD, DH and LFT were measured in mm, DSCA in mm^2, respectively, while LA in degree. All measurements were kept to one decimal place.

Image quality assessment

All image quality was assessed by two readers using a Likert 5-point scale: score 5, the main structures were perfectly displayed, no artifacts or imaging distortion, no effect on diagnosis; score 4, well displayed structures, few artifacts, slight image distortion, little effect on diagnosis; score 3, relatively well displayed, a few artifacts, slight image distortion, a certain effect on diagnosis; score 2, moderate displayed structures, moderate artifacts and image distortion, significant effect on diagnosis; score 1, severe artifacts, image distortion, or poor signal intensity, unavailable for diagnosis. The image quality score is performed by the reading physician at the same time as each image measurement.

Examinee comfort assessment

After every MRI scanning, patients were asked to assess the level of comfort of the examinations on a Likert 5-point scale: score 5, no discomfort during the examination; score 4, only mild discomfort during the examination; score 3, certain discomfort, but examination can be done easily; score 2, obvious discomfort, but examination can be done difficultly; score 1, intolerable discomfort, and examination could not be done (examinations that were not completed due to patient intolerance were counted as score 1). After all examinations were completed, patients were asked to revise their scores for each examination. We also interviewed patients with score 3 and below about the reasons for their discomfort.

Image interpretation

All images were read by two radiologists with 14 and 7 years of experience in reading lumbar spine MRI imaging respectively. All parameters were measured using a workstation (AW, version 4.6, GE Medical Systems). The MRI images were sent to the radiologists with the types of examinations and details of the participants' information withheld.

When measuring quantitative parameters, the images are magnified to the appropriate extent to ensure the accuracy. All quantitative parameters were measured three times by each reader and averaged, with each measurement taken 3 days apart. The final quantitative data used was the average of the values measured by the two readers. If the quantitative values difference were more than 10% or the results of the qualitative indicators are inconsistent, an agreement will be reached after consultation by two readers.

Statistical analysis

The statistical analyses were performed using the software SPSS 25.0 (IBM Corp., Armonk, NY, USA). The cohort was characterized using means and standard deviations to describe continuous variables and proportions to describe categorical variables. Differences in LA, DSCA, DH and LFT in 4 examinations were compared using repeated measures analysis of variance (ANOVA), and Bonferroni post hoc correction was used to analyze which of the pairways comparisons from an ANOVA are significant. Image quality was compared using the Friedman test followed by the Dunn test for multiple comparisons. Inter-observer and intra-observer reliability for the quantitative parameters assessment were calculated by the intraclass correlation coefficient (ICC). Absolute agreement, two-way random effects, and single measure models were adopted. 95% CIs were calculated with bootstrapping. Statistical significance was defined as $p < 0.05$. The ICC values <0.4, between 0.4 and 0.54, between 0.55 and 0.69, between 0.70 and 0.84, and exceeding 0.85 represented poor, weak, moderate, good, and excellent agreement, respectively [17].

Result

Study population

A total of 40 symptomatic patients were included in the study. The baseline characteristics and clinical symptoms are summarized in Table 2. All 40 patients successfully completed rMRI. 3 patients were unable to tolerate eMRI, but they all completed r+alMRI. 1 patient was unable to tolerate r+alMRI as well as e+alMRI, and 4 patients were unable to tolerate e+alMRI. 35 patients finally completed all 4 examinations (Fig. 3).

Table 2 Baseline characteristics and clinical symptoms of the patients

Baseline Characteristics	
Age (yr)	55.3 ± 9.6
Sex (female)	17 (42.5)
Height (cm)	170.1 ± 7.6
Body weight (kg)	68.4 ± 10.0
Body mass index (kg/m^2)	23.6 ± 2.8
Symptoms	
Duration of symptoms (mo)	30.4 ± 31.9
Intermittent claudication	27 (67.5)
Leg pain	33 (82.5)
Leg numbness	31 (77.5)
Low back pain	36 (90)

Data are mean±SD or n (%)

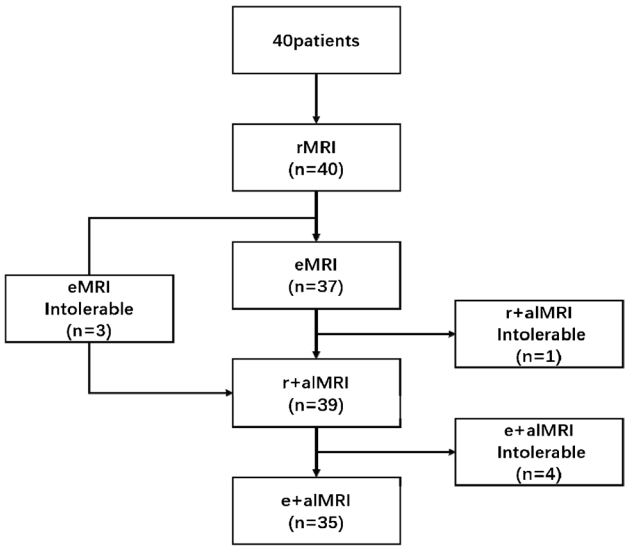

Fig. 3 Study flowchart for patients undergoing 4 examinations. rMRI, psoas-relaxed position MRI; eMRI, extended position MRI; r+alMRI, the psoas-relaxed position axial loading MRI; e+alMRI, the extended position axial loading MRI

Comparison of quantitative parameters

The mean value of DSCA, SVCD, DH, LFT and LA for 40 patients are listed in Table 3.

The DSCA values among the 4 examinations are shown in Fig. 4A. Compared to rMRI, a statistically significant reduction in DSCA was found only at the L4-5 level ($p = 0.033$) in eMRI, but not at the L3-4 and L5-S1. However, a statistically significant decrease was observed at all levels (L3-4, $p = 0.041$; L5-S1, $p = 0.005$; L4-5, $p = 0.002$) in r+alMRI, with a further decrease at all levels in e+alMRI (all $p < 0.001$) (Fig. 5).

The SVCD and DH values among the 4 examinations are shown in Fig. 4B and C. Compared to rMRI, eMRI did not show statistically significant difference at all levels, r+alMRI showed statistically significant reductions at the L3-4 ($p = 0.018$) and L4-5 for SVCD ($p = 0.011$) and all levels for DH (L3-4, $p = 0.027$; L5-S1, $p = 0.001$; L4-5, $p < 0.001$), while e+alMRI showed statistically significant reductions at all levels for SVCD and DH ($p < 0.001$).

The LFT values among the 4 examinations are shown in Fig. 4D and had a statistically significant increase in the extension position compared to the psoas-relaxed position ($p < 0.001$). The LFT was thicker in eMRI compared to r+alMRI at all levels (L3-4, $p = 0.038$; L5-S1, $p = 0.012$; L4-5, $p = 0.002$).

The LA in extended position had a statistically significant increase compared to the psoas-relaxed position with or without axial loading (Fig. 4E, $p < 0.001$).

The inter-observer ICCs for DSCA, SVCD, DH, LFT and LA were 0.950 (95% CI 0.894 to 0.969), 0.911 (95% CI 0.822 to 0.958), 0.898 (95% CI 0.831 to 0.964), 0.739

Table 3 qualitative parameters among 4 examinations

	rMRI	eMRI	r+alMRI	e+alMRI	F*	*p**
DSCA (mm^2)						
L3-4	123.25±16.19	115.73±15.32	113.68±14.64	109.91±14.64	4.828	0.003
L4-5	92.94±8.69	87.09±7.54	85.47±8.68	81.50±11.34	10.267	0.000
L5-S1	95.74±7.30	93.31±6.67	90.41±7.30	90.41±9.47	7.468	0.000
SVCD (mm)						
L3-4	9.94±1.87	9.58±1.86	8.61±2.02	8.33±2.03	5.827	0.001
L4-5	8.70±1.93	8.41±1.85	7.45±2.03	7.08±1.97	5.832	0.001
L5-S1	8.90±1.81	8.70±1.83	7.92±1.85	7.62±1.91	4.082	0.008
DH (mm)						
L3-4	8.13±0.59	8.06±0.56	7.74±0.53	7.60±0.69	6.555	0.000
L4-5	8.81±0.55	8.63±0.59	8.18±0.73	8.11±0.73	10.284	0.000
L5-S1	8.38±0.55	8.27±0.52	7.88±0.60	7.84±0.57	9.146	0.000
LFT (mm)						
L3-4	2.68±0.46	3.10±0.59	2.77±0.51	3.17±0.55	7.942	0.000
L4-5	2.98±0.44	3.50±0.53	3.10±0.44	3.58±0.49	14.642	0.000
L5-S1	2.29±0.42	2.70±0.45	2.39±0.42	2.74±0.44	10.196	0.000
LA (degree)	34.64±11.51	43.20±11.84	36.37±11.18	45.04±11.86	7.220	0.000

Data represented as mean±SD. DSCA, dural-sac cross-sectional area; SVCD, sagittal vertebral canal diameter; *DH* disc height, *LFT* ligamentum flavum thickness, *LA* lordosis angle, *rMRI* psoas-relaxed position MRI, *eMRI* extended position MRI, r+alMRI the psoas-relaxed position axial loading MRI, e+alMRI the extended position axial loading MRI. *F and p values were calculated with repeated measures ANOVA among the four MRIs

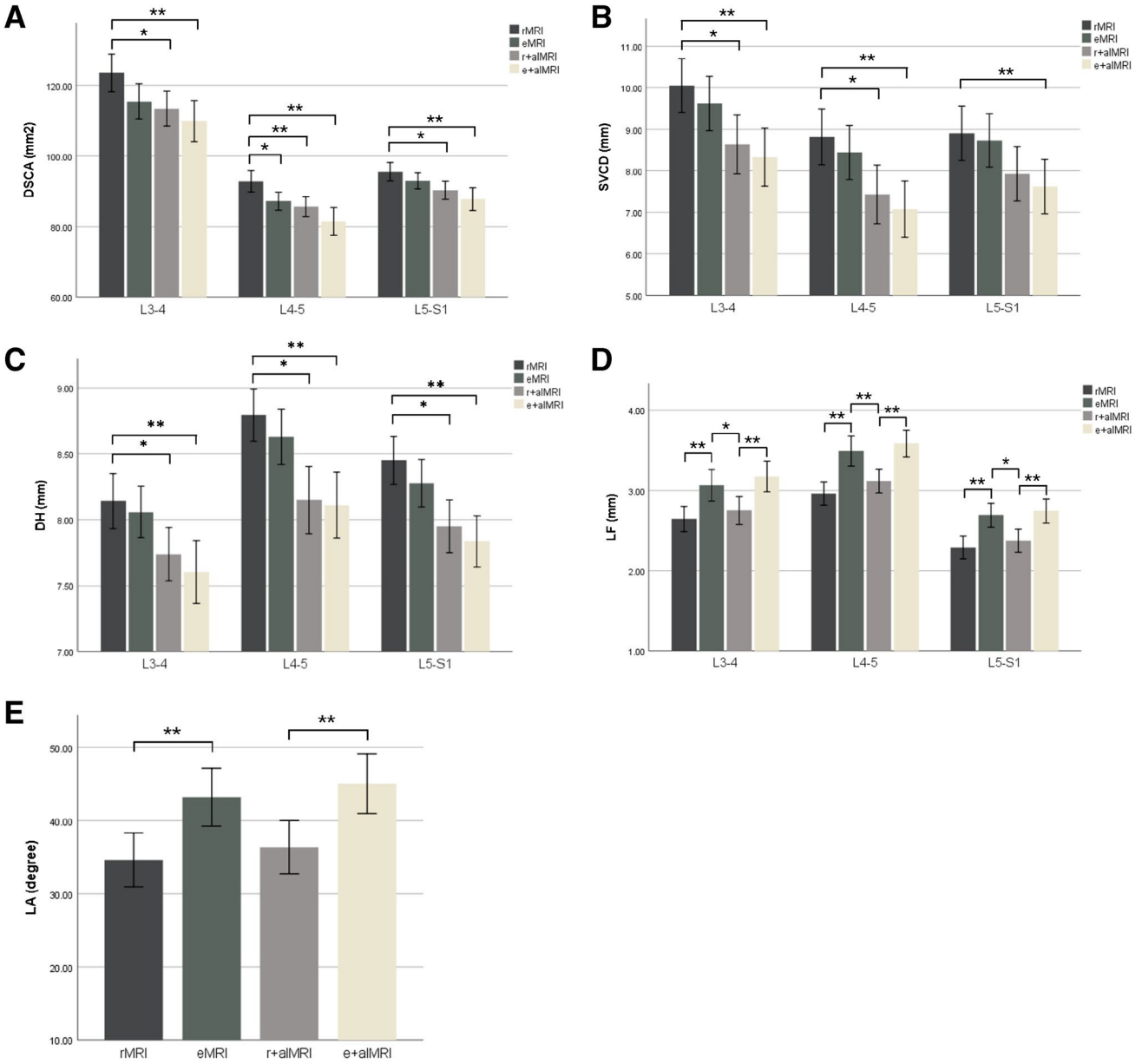

Fig. 4 Comparison of DSCA(**A**), SVCD (**B**), DH (**C**), LFT (**D**) at L3-L4, L4-L5, L5-S1 and LA (**E**) of L1-S1. Data are the means ± SD. *$p < 0.05$, ** $p < 0.01$. DSCA, dural-sac cross-sectional area; SVCD, sagittal vertebral canal diameter; DH, disc height; LFT, ligamentum flavum thickness; LA, lordosis angle; FRFSE, fast recovery fast spin-echo. rMRI, psoas-relaxed position MRI; eMRI, extended position MRI; r+alMRI, the psoas-relaxed position axial loading MRI; e+alMRI, the extended position axial loading MRI

(95% CI 0.567 to 0.819) and 0.884 (95% CI 0.819 to 0.959), respectively, suggesting good to excellent reliability.

The intra-observer ICCs for DSCA, SVCD, DH, LFT and LA were 0.987 (95% CI 0.935 to 0.994), 0.960 (95% CI 0.909 to 0.986), 0.921 (95% CI 0.853 to 0.962), 0.833 (95% CI 0.682 to 0.895) and 0.915 (95% CI 0.841 to 0.948), suggesting good to excellent reliability. The full reliability analysis are presented in Table 4.

Image quality assessment

The scores of image quality assessment for the 4 examinations are listed in Table 5, and the mean scores for the 4 examinations were 4.88±0.00,4.76±0.01, 4.79±0.01 and 4.69±0.17, respectively. There were with no statistical difference between the image quality of the 4 examinations ($p = 0.124$).

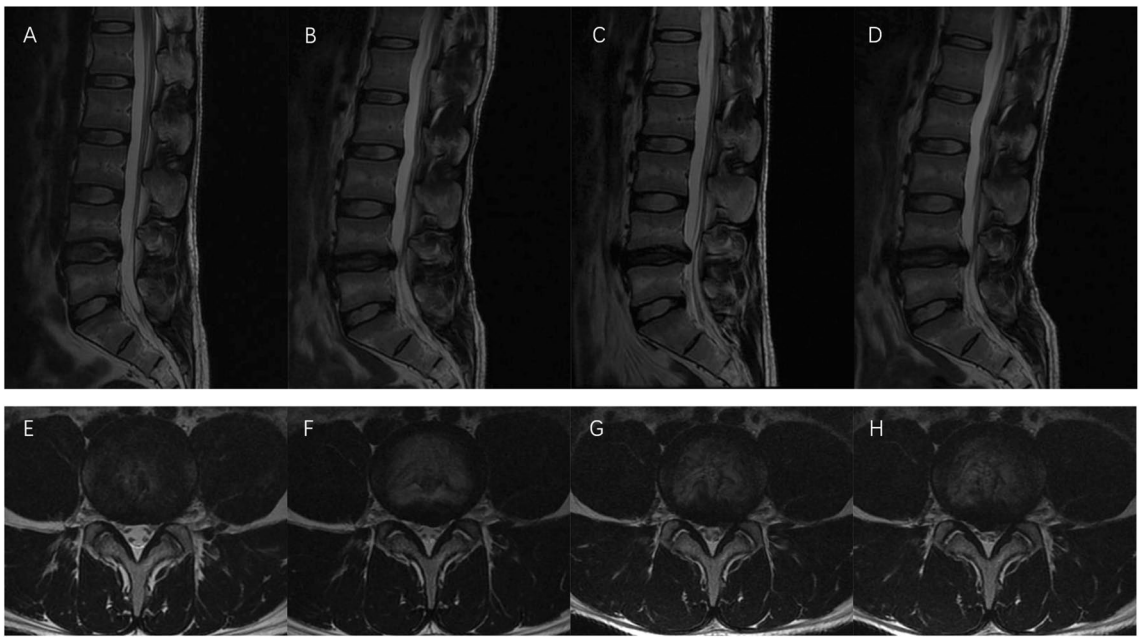

Fig. 5 A 34-year-old man. Sagittal T2-weighted fast recovery fast spin-echo (FRFSE) (**A, B, C, D**) and axial T2-weighted FRFSE of (**E, F, G, H**) of rMRL (**A, E**), eMRI (B, F), r+alMRI (**C, G**) and e+alMRI (**D, H**). Relative to rMRI, spinal stenosis in L4-5 aggravated progressively in the other three examinations. DSCA was 115.3mm^2, 86.3 mm^2, 73.2 mm^2 and 63.1 mm^2 in rMRI, eMRI, r+alMRI and e+alMRI, respectively. rMRI, psoas-relaxed position MRI; eMRI, extended position MRI; r+alMRI, the psoas-relaxed position axial loading MRI; e+alMRI, the extended position axial loading MRI; DSCA, dural-sac cross-sectional area

Table 4 Inter- and intra-observer ICCs for quantitative parameters between examinations

	Inter-observer	Intra-observer
DSCA	0.950 (0.894-0.969)	0.987 (0.935-0.994)
SVCD	0.911 (0.822-0.958)	0.960 (0.909-0.986)
DH	0.898 (0.831-0.964)	0.921 (0.853-0.962)
LFT	0.739 (0.567-0.819)	0.833 (0.682-0.895)
LA	0.884 (0.819-0.959)	0.915 (0.841-0.948)

ICC intraclass correlation coefficient, *DSCA* dural-sac cross-sectional area, *SVCD* sagittal vertebral canal diameter, *DH* disc height, *LFT* ligamentum flavum thickness, *LA* lordosis angle

Data are ICC values, with 95% CI in parentheses. The inter-observer reliability is based on each reader's measurement of all quantitative parameters for each patient. The intra-observer reliability is based on each reader's three measurements of the quantitative parameters

Examinee comfort assessment

The scores of examinee comfort assessment for the 4 examinations are listed in Table 6, and the mean scores for the 4 examinations were 4.33±0.69,3.90±1.26, 3.98±1.05 and 3.65±1.39, respectively. Compared to rMRI, examinee comfort scores were decreased in both eMRI and r+alMRI, and with a statistically significant decrease in e+alMRI (p = 0.004).

All patients with scores of 1or 2 were due to increased pain or numbness in the low back and legs after extension or axial loading of the lumbar spine. Patients with scores of 3 had the above reasons besides the complaints of MRI noise during the examination or/and mild claustrophobia in

Table 5 Image quality assessment among 4 examinations, no. (%)

score	rMRI, *n*=40	eMRI, *n*=37	r+alMRI, *n*=39	e+alMRI, *n*=35
5	34 (85.0)	30 (81.1)	33 (84.6)	28 (80.0)
4	5 (12.5)	5 (13.5)	4 (10.3)	4 (11.4)
3	1 (2.5)	2 (5.4)	2 (5.1)	2 (5.7)
2	0 (0)	0 (0)	0 (0)	1 (2.9)
1	0 (0)	0 (0)	0 (0)	0 (0)
Mean (± SD)	4.83±0.45	4.76±0.55	4.79±0.52	4.69±0.72

rMRI psoas-relaxed position MRI, *eMRI* extended position MRI, r+alMRI the psoas-relaxed position axial loading MRI, *e+alMRI* the extended position axial loading MRI

Table 6 Examinee comfort assessment among 4 examinations, no. (%)

score	rMRI, *n*=40	eMRI, *n*=40	r+alMRI, *n*=40	e+alMRI, *n*=40
5	18 (45.0)	18 (45.0)	16 (40.0)	15 (37.5)
4	17 (42.5)	8 (20.0)	11(37.5)	9 (22.5)
3	5 (12.5)	9 (22.5)	10(25.0)	8 (20.0)
2	0 (0)	2 (5.0)	2 (5.0)	3 (7.5)
1	0 (0)	3(7.5)	1 (2.5)	5 (12.5)
Mean (± SD)	4.33±0.69	3.90±1.26	3.98±1.05	3.65±1.39*

Post hoc comparison showed a significant difference between rMRI and e+alMRI (p = 0.004). rMRI, psoas-relaxed position MRI; eMRI, extended position MRI; r+alMRI, the psoas-relaxed position axial loading MRI; e+alMRI, the extended position axial loading MRI

3 patients. No patients complained of discomfort from the axial loading device.

Disscusion

The mechanism of the previous axial loading device, which applies pressure through the shoulders and feet, required that the lumbar spine must be in the extended position during the examination to ensure stability. Therefore, it is not possible to distinguish the effects between axial loading and extension on LSS. In previous studies, we have demonstrated that the new device provides more diagnostic information for patients with spinal stenosis and has good stability and repeatability [11, 12]. An advantage of the new device is to allow for a kinetic examination in different positions of lumbar spine such as lumbar spine extended or psoas-relaxed position. In this study, we found that both axial loading and positions affected LSS, however, the pattern of influence was different.

The DSCA was the most accurate parameter for evaluating LSS and reflected the severity of LSS directly [18, 19]. A significant reduction in DSCA after axial loading was considered a meaningful change, and previous studies have found that patients with this sign had more severe clinical symptoms [20, 21]. Compared to rMRI, both eMRI and r+alMRI showed a decrease in DSCA, while r+alMRI showed a greater decrease than eMRI. During eMRI, only L4-5 showed a statistically significant decrease in DSCA, which was found at all 3 levels during r+alMRI. It suggests that axial loading has a greater effect on LSS compared to extended position. Meanwhile, e+alMRI further aggravated the severity of LSS.

In the DH and SVCD, only alMRI showed a statistically significant decrease compared to rMRI. These two parameters represented flattening and posterior herniation or bulging of the lumbar disc after compression [22–24]. The decrease in DH and SVCD explained that alMRI affected the morphology of the lumbar intervertebral disc by axial compression.

This study showed a statistically significant increase in LFT only in the extended position rather than in axial loading. We speculated that the main cause of the increased LFT was the buckling of the ligamentum flavum due to extension. This speculation was consistent with other studies, which suggested that the increase in LFT was mainly due to in-folding and bending of the ligamentum flavum into the spinal canal [25, 26].

Of the 4 examinations, e+alMRI showed the greatest variation in all quantitative parameters. Compared with rMRI, the DSCA, SVCD, DH and LFT showed statistically significant changes at all three intervertebral levels. These results were consistent with studies using Dynawell, and these changes in quantitative parameters may led to measurable advancement in the diagnosis of LSS [5, 27]. These changes may potentially change the strategy for the next step in treatment. In a study, after three neurosurgeons read the alMRI images and comprehensively analyzed the patients' condition, treatment was changed from conservative treatment to decompression surgery for five of the 20 patients [28].

However, an important issue with e+alMRI is the comfort of the patient with the examination. There was a statistically significant reduction in patient comfort scores with e+alMRI compared to rMRI. In this study, of the consecutive 40 patients, 5 could not tolerate e+alMRI. Even for eMRI, 3/40 will patients could not tolerate the examination, while for r+alMRI, only 1/40 could not tolerate it. All three patients who could not tolerate eMRI complained of significantly increased low back pain during the examination. We hypothesized that the reason for the increased low back pain might be related to the increased pressure on the posterior lumbar spine. In eMRI, the LFTs at all three intervertebral levels were thicker than those in alMRI, suggesting that the posterior lumbar compression was more pronounced. Some studies have demonstrated that degeneration and inflammation of the posterior lumbar joints are an important reason for low back pain [29, 30]. In a study of lumbar spine extended position MRI, 2/44 patients were unable to tolerate the lumbar spine extended position [10]. Some studies using Dynawell have mentioned that patients might not tolerate

the examination, but no studies have yet evaluated examinee comfort [5, 31]. Interestingly, some patients who felt discomfort were more concerned with the discomfort of the MRI itself rather than the axial loading device or extension, such as noise and claustrophobia [32, 33].

There might be safety and efficiency issues during the examination using Dynawell. If patients could not tolerate, the technician need to take time to return to the examination bed and adjust a manual rotating knob to release or adjust the pressure [16, 34–38]. These problems are resolved with our new device which adopts a pneumatic mode that allows pressure release and regulation remotely.

This study had some limitations. First, some patients may not achieve maximum extension of the lumbar spine during the examination. Although we used a thick cushion with memory foam to ensure that it adapts as much as possible to the different patients' lumbar spine. However, the conclusions drawn from the study were still persuasive. Second, for patients with thick back fat, the cushion could cause a distinct pressure mark recognizable resulting in the readers not being fully blinded to the examinations. Third, we only compared some basic quantitative parameters but lacked some semi-quantitative and qualitative data such as foraminal stenosis, disc herniation.

In conclusion, both axial loading and extension of lumbar spine could exacerbate LSS, but the mechanisms may be different. In patients with suspected LSS, e+alMRI can provide more information for diagnosis, and in patients who cannot tolerate e+alMRI, r+alMRI may be a good choice.

Funding This study was supported by the General Program of the Special Project of Military Health Care (No. 18BJZ43).

Data availability The datasets used and/or analysed during the current study available from the corresponding author on reasonable request.

Declarations

Competing interests The authors declare no competing interests.

References

1. Katz JN, Zimmerman ZE, Mass H, Makhni MC. Diagnosis and Management of Lumbar Spinal Stenosis: A Review. JAMA. 2022;327(17):1688–99.
2. Kreiner DS, Shaffer WO, Baisden JL, et al. An evidence-based clinical guideline for the diagnosis and treatment of degenerative lumbar spinal stenosis (update). Spine J. 2013;13(7):734–43.
3. Charoensuk J, Laothamatas J, Sungkarat W, Worapruekjaru L, Hooncharoen B, Chousangsuntorn K. Axial loading during supine MRI for improved assessment of lumbar spine: comparison with standing MRI. Acta Radiol. 2023;64(1):217–227.
4. Hioki A, Miyamoto K, Sakai H, Shimizu K. Lumbar axial loading device alters lumbar sagittal alignment differently from upright standing position: a computed tomography study. Spine (Phila Pa 1976). 2010;35(9):995–1001.
5. Kim YK, Lee JW, Kim HJ, Yeom JS, Kang HS. Diagnostic advancement of axial loaded lumbar spine MRI in patients with clinically suspected central spinal canal stenosis. Spine (Phila Pa 1976). 2013;38(21):E1342–7.
6. Sasani H, Solmaz B, Sasani M, Vural M, Ozer AF. Diagnostic Importance of Axial Loaded Magnetic Resonance Imaging in Patients with Suspected Lumbar Spinal Canal Stenosis. World Neurosurg. 2019;127:e69–75.
7. Hebelka H, Rydberg N, Hutchins J, Lagerstrand K, Brisby H. Axial Loading during MRI Induces Lumbar Foraminal Area Changes and Has the Potential to Improve Diagnostics of Nerve Root Compromise. J Clin Med. 2022;11(8):2122.
8. Kanno H, Aizawa T, Ozawa H, Koizumi Y, Morozumi N, Itoi E. An increase in the degree of olisthesis during axial loading reduces the dural sac size and worsens clinical symptoms in patients with degenerative spondylolisthesis. Spine J. 2018;18(5):726–33.
9. Madsen R, Jensen TS, Pope M, Sørensen JS, Bendix T. The effect of body position and axial load on spinal canal morphology: an MRI study of central spinal stenosis. Spine (Phila Pa 1976). 2008;33(1):61–7.
10. Hansen BB, Hansen P, Grindsted J, et al. Conventional Supine MRI With a Lumbar Pillow-An Alternative to Weight-bearing MRI for Diagnosing Spinal Stenosis?: A Cross-sectional Study. Spine (Phila Pa 1976). 2017;42(9):662–9.
11. Fang X, Li J, Liu L, Zhang Y, Tang Z, Zhang J. Axial loading lumbar magnetic resonance imaging with a new device in asymptomatic individuals. Quant Imaging Med Surg. 2023;13(1):58–65.
12. Fang X, Li J, Wang L, et al. Diagnostic value of a new axial loading MRI device in patients with suspected lumbar spinal stenosis. Eur Radiol. 2023;33(5):3200–10.
13. Sato K, Kikuchi S, Yonezawa T. In vivo intradiscal pressure measurement in healthy individuals and in patients with ongoing back problems. Spine (Phila Pa 1976). 1999;24(23):2468–74.
14. Willén J, Danielson B. The diagnostic effect from axial loading of the lumbar spine during computed tomography and magnetic resonance imaging in patients with degenerative disorders. Spine (Phila Pa 1976). 2001;26(23):2607–14.
15. Hebelka H, Torén L, Lagerstrand K, Brisby H. Axial loading during MRI reveals deviant characteristics within posterior IVD regions between low back pain patients and controls. Eur Spine J. 2018;27(11):2840–6.
16. Torén L, Hebelka H, Kasperska I, Brisby H, Lagerstrand K. With axial loading during MRI diurnal T2-value changes in lumbar discs are neglectable: a cross sectional study. BMC Musculoskelet Disord. 2018;19(1):25.
17. Schober P, Mascha EJ, Vetter TR. Statistics From A (Agreement) to Z (z Score): A Guide to Interpreting Common Measures of Association, Agreement, Diagnostic Accuracy, Effect Size, Heterogeneity, and Reliability in Medical Research. Anesth Analg. 2021;133(6):1633–41.
18. Lurie J, Tomkins-Lane C. Management of lumbar spinal stenosis. BMJ. 2016;352:h6234.
19. Andreisek G, Hodler J, Steurer J. Uncertainties in the diagnosis of lumbar spinal stenosis. Radiology. 2011;261(3):681–4.
20. Kanno H, Ozawa H, Koizumi Y, et al. Dynamic change of dural sac cross-sectional area in axial loaded magnetic resonance imaging correlates with the severity of clinical symptoms in patients with lumbar spinal canal stenosis. Spine (Phila Pa 1976). 2012;37(3):207–13.
21. Ozawa H, Kanno H, Koizumi Y, et al. Dynamic changes in the dural sac cross-sectional area on axial loaded MR imaging: is there a difference between degenerative spondylolisthesis and spinal stenosis. AJNR Am J Neuroradiol. 2012;33(6):1191–7.
22. Steurer J, Roner S, Gnannt R, Hodler J. LumbSten Research Collaboration. Quantitative radiologic criteria for the diagnosis of

lumbar spinal stenosis: a systematic literature review. BMC Musculoskelet Disord. 2011;12:175.
23. Vamvanij V, Ferrara LA, Hai Y, Zhao J, Kolata R, Yuan HA. Quantitative changes in spinal canal dimensions using interbody distraction for spondylolisthesis. Spine (Phila Pa 1976). 2001;26(3):E13–8.
24. Pfirrmann CW, Metzdorf A, Zanetti M, Hodler J, Boos N. Magnetic resonance classification of lumbar intervertebral disc degeneration. Spine (Phila Pa 1976). 2001;26(17):1873–8.
25. Altinkaya N, Yildirim T, Demir S, Alkan O, Sarica FB. Factors associated with the thickness of the ligamentum flavum: is ligamentum flavum thickening due to hypertrophy or buckling. Spine (Phila Pa 1976). 2011;36(16):E1093–7.
26. Yabe Y, Hagiwara Y, Tsuchiya M, et al. Factors Associated with Thickening of the Ligamentum Flavum on Magnetic Resonance Imaging in Patients with Lumbar Spinal Canal Stenosis. Spine (Phila Pa 1976). 2022;47(14):1036–41.
27. Kinder A, Filho FP, Ribeiro E, et al. Magnetic resonance imaging of the lumbar spine with axial loading: a review of 120 cases. Eur J Radiol. 2012;81(4):e561–4.
28. Hiwatashi A, Danielson B, Moritani T, et al. Axial loading during MR imaging can influence treatment decision for symptomatic spinal stenosis. AJNR Am J Neuroradiol. 2004;25(2):170–4.
29. Rousseau MA, Lazennec JY. Degenerative disease supra- and infra-jacent to fused lumbar and lumbo-sacral levels. Orthop Traumatol Surg Res. 2016;102(1 Suppl):S1–8.
30. Gellhorn AC, Katz JN, Suri P. Osteoarthritis of the spine: the facet joints. Nat Rev Rheumatol. 2013;9(4):216–24.
31. Huang KY, Lin RM, Lee YL, Li JD. Factors affecting disability and physical function in degenerative lumbar spondylolisthesis of L4-5: evaluation with axially loaded MRI. Eur Spine J. 2009;18(12):1851–7.
32. Enders J, Zimmermann E, Rief M, et al. Reduction of claustrophobia during magnetic resonance imaging: methods and design of the "CLAUSTRO" randomized controlled trial. BMC Med Imaging. 2011;11:4.
33. Price DL, De Wilde JP, Papadaki AM, Curran JS, Kitney RI. Investigation of acoustic noise on 15 MRI scanners from 0.2 T to 3 T. J Magn Reson Imaging. 2001;13(2):288–93.
34. Nilsson M, Lagerstrand K, Kasperska I, Brisby H, Hebelka H. Axial loading during MRI influences T2-mapping values of lumbar discs: a feasibility study on patients with low back pain. Eur Spine J. 2016;25(9):2856–63.
35. Hioki A, Miyamoto K, Shimizu K, Inoue N. Test-retest repeatability of lumbar sagittal alignment and disc height measurements with or without axial loading: a computed tomography study. J Spinal Disord Tech. 2011;24(2):93–8.
36. Hjaltadottir H, Hebelka H, Molinder C, Brisby H, Baranto A. Axial loading during MRI reveals insufficient effect of percutaneous interspinous implants (Aperius™ PerCLID™) on spinal canal area. Eur Spine J. 2020;29(1):122–8.
37. Nordberg CL, Hansen BB, Nybing JD, et al. Weight-bearing MRI of the Lumbar Spine: Technical Aspects. Semin Musculoskelet Radiol. 2019;23(6):609–20.
38. Fiani B, Griepp DW, Lee J, Davati C, Moawad CM, Kondilis A. Weight-Bearing Magnetic Resonance Imaging as a Diagnostic Tool That Generates Biomechanical Changes in Spine Anatomy. Cureus. 2020;12(12):e12070.